Published in final edited form as:
J Mol Biol. 2012 October 26; 423(3): 303–314. doi:10.1016/j.jmb.2012.07.009.

The Primary and Secondary Translocase Activities within *E. coli* RecBC Helicase are Tightly Coupled to ATP hydrolysis by the RecB Motor

Colin G. Wu[1], **Fuqian Xie**, and **Timothy M. Lohman**[*]
Department of Biochemistry and Molecular Biophysics, Washington University School of Medicine, 660 S. Euclid Avenue, Box 8231, Saint Louis, MO 63110

Abstract

E. coli RecBC, a rapid and processive DNA helicase with only a single ATPase motor (RecB), possesses two distinct single stranded (ss)DNA translocase activities that can operate on each strand of an unwound duplex DNA. Using a transient kinetic assay to detect phosphate release, we show that RecBC hydrolyzes the same amount of ATP when translocating along ssDNA using only its primary (0.81 ± 0.05 ATP/nt), only its secondary (1.12 ± 0.06 ATP/nt), or both translocases simultaneously (1.07 ± 0.09 ATP/nt). A mutation within RecB (Y803H) that slows the primary translocation rate of RecBC also slows the secondary translocation rate to the same extent. These results indicate that the ATPase activity of the single RecB motor drives both the primary and secondary RecBC translocases in a tightly coupled reaction. We further show that RecBC also hydrolyzes the same amount of ATP (0.95 ± 0.08 ATP/bp) while processively unwinding duplex DNA suggesting that the large majority, possibly all, of the ATP hydrolyzed by RecBC during DNA unwinding is used to fuel ssDNA translocation rather than to facilitate base pair melting. A model for DNA unwinding is proposed based on these observations.

Keywords

translocation kinetics; recombination; double strand break repair; allostery; unwinding mechanism

Introduction

DNA helicases are a ubiquitous class of motor proteins that function by coupling nucleoside triphosphate (NTP) binding and hydrolysis to unwind duplex DNA to produce the transient single stranded (ss) DNA intermediates required for all aspects of DNA metabolism.[1–6] The *E. coli* RecBCD enzyme possesses DNA helicase and nuclease activities, and is involved in the major pathway of homologous recombination in *E. coli.* [7–10] In particular, RecBCD functions to repair damage induced double stranded (ds) DNA breaks. This heterotrimer

[*]Address correspondence to: Timothy M. Lohman, Department of Biochemistry and Molecular Biophysics, Washington University School of Medicine, 660 S. Euclid Avenue, Box 8231, Saint Louis, MO 63110, (314)-362-4393, (314)-362-7183, (Fax) lohman@biochem.wustl.edu.
[1]Current address: Department of Biochemistry, University of Illinois, Urbana, IL 61801

Conflict of Interest
The authors declare that they have no conflict of interest.

possesses two superfamily-1 (SF1) ATPase motors: RecB (134 kDa), a 3′ to 5′ helicase/translocase, and RecD (67 kDa), a 5′ to 3′ helicase/translocase.[11–14] RecC (129 kDa) is structurally similar to RecB but devoid of the amino acids required for ATP binding and functions instead as a processivity and regulatory factor.[15]

Although the two ATPase motors have opposite ssDNA translocation directionalities, they function within RecBCD to unwind dsDNA in the same net direction by translocating along the complementary strands of the DNA duplex. RecBCD first binds to the damaged DNA at a blunt or nearly blunt end and then unwinds the duplex in an ATP-dependent manner with RecD serving as the lead motor. Two models have been proposed for how RecBCD promotes formation of a RecA filament. In one model, during unwinding RecBCD preferentially degrades the 3′ terminated DNA strand while cleaving the 5′ terminated strand infrequently.[17–19] These activities continue until RecBCD recognizes the “crossover hotspot instigator” (chi) regulatory sequence (5′-GCTGGTGG-3′) within the unwound ssDNA, whereupon RecBCD continues to unwind the DNA, but at a slower rate with RecB now acting as the faster lead motor. After chi recognition the nuclease activity is also modified such that it now preferentially degrades the 5′ terminated ssDNA, thereby creating a 3′ ssDNA overhang onto which RecBCD can load the RecA protein.[21–23] The resulting RecA-ssDNA filament initiates recombinational repair of the DNA break. In a second model,[24] the nuclease activity is inactive until chi recognition occurs, at which point a nick is introduced in the 3′ terminated strand, followed by RecA loading at the nick.

The RecBC enzyme, without the RecD subunit, still functions as a rapid and processive helicase with a greatly attenuated nuclease activity.[25–27] Since RecBC possesses a single ATPase motor (RecB), this simpler enzyme is a good model system to study how ATP binding and hydrolysis is coupled to DNA unwinding and translocation, and may serve as a model for RecBCD after “chi” recognition. RecBC can “melt-out” six base pairs upon DNA binding in a Mg^{2+} dependent but ATP independent manner and thus binds with optimal affinity to DNA ends with pre-existing 5′-$(dT)_6$ and 3′-$(dT)_6$ ssDNA tails.[28–30]

Wu et al. [31] have recently shown that RecBC (without RecD) possesses two distinct translocase activities that are controlled by the single ATPase motor within RecB as depicted schematically in Fig. 1. The primary translocase enables RecBC to translocate along ssDNA in the expected 3′ to 5′ direction, consistent with the directional motion of RecB alone on ssDNA, while a secondary translocase activity facilitates translocation along the other DNA strand, although the secondary translocase is not sensitive to the polarity of the ssDNA backbone.[31] As such, RecBC can use both translocase activities to move simultaneously along two non-complementary strands of ssDNA.

To better understand the relationship between the primary and secondary ssDNA translocase activities within RecBC, we measured ATP consumption (coupling stoichiometry) during RecBC translocation along ssDNA using only its primary translocase, only its secondary translocase or both. The results demonstrate that the RecB ATPase drives both translocase activities simultaneously in a highly coupled allosteric process.

Results

DNA substrate design

The DNA substrates used to measure ATP hydrolysis during ssDNA translocation by RecBC are shown schematically in Fig. 2a, b and Fig. 3a. Each possesses a high affinity RecBC loading site (5′-$(dT)_6$, 3′-$(dT)_6$ ssDNA tails) [32] at one end of a duplex region of constant length (24 bp), followed by a ssDNA ($(dT)_L$) extension of either one or both strands (L = 15, 30, 45, 60, or 75 nucleotides (nts)). The DNA substrates in Fig. 2a, b and 3a were

used to examine RecBC translocation using only its primary translocase, only its secondary translocase, or both translocases simultaneously, respectively. RecBC binds only to the high affinity loading site when DNA is present in excess (200 nM) over RecBC (20 nM) and initiates unwinding of the 24 bp duplex region upon addition of ATP. Specific binding of RecBC at the high affinity loading site is also ensured by the fact that the affinity of RecBC for a DNA end decreases dramatically for ends with a 3′ ssDNA tail length greater than six nucleotides. As shown previously,[31] after RecBCD unwinds the 24 bp duplex, it will continue to translocate along the $(dT)_L$ ssDNA extensions. Hence, the total amount of ATP hydrolysis measured will be due to RecBC unwinding of the constant length (24 bp) duplex DNA and subsequent translocation along the ssDNA ($(dT)_L$) extension(s), and the slope of a plot of the extent of ATP hydrolysis versus ssDNA extension length, *L*, yields the ATP consumption per nucleotide translocated by RecBC.

ATP hydrolysis by RecBC during ssDNA translocation using only its primary translocase

We examined the kinetics of ATP hydrolysis during ssDNA translocation by RecBC using a stopped-flow fluorescence assay that measures release of inorganic phosphate upon ATP hydrolysis.[34] This method utilizes the A197C mutant of *E. coli* phosphate binding protein (PBP), labeled fluorescently with coumarin (MDCC) that exhibits a large increase in coumarin fluorescence when it binds inorganic phosphate. This probe has been used to examine the ATPase activity of a number of helicases and translocases.[35–40] Phosphate release experiments were performed as described in Materials and Methods.

RecBC (20 nM) was pre-mixed with an excess of each DNA substrate (200 nM) in one syringe of the stopped-flow in Buffer M at 25°C. Reactions were then initiated by 1:1 mixing with 150 μM ATP, 10 mg/mL heparin trap, and 40 μM PBP-MDCC. Final concentrations after mixing were therefore 100 nM DNA, 10 nM RecBC, 75 μM ATP, 5 mg/mL heparin, and 20 μM PBP-MDCC in Buffer M. All experiments were performed at low [ATP] (75 μM) to minimize the amount of phosphate binding protein (PBP-MDCC) used. Experiments performed in the absence of DNA were used to determine the amount of phosphate contamination within the buffers and reagents, and to measure any background ATP hydrolysis. Calibration of the PBP-MDCC fluorescence change (see Materials and Methods) was performed by mixing the ATP, heparin, and PBP-MDCC solution with known concentrations of inorganic phosphate (Supplementary Fig. 1). Control experiments indicate that under these conditions, PBP-MDCC binding to phosphate is not rate limiting, and heparin does not stimulate the ATPase activity of RecBC.

To examine the ATP coupling of RecBC while translocating using only its primary (3′ to 5′) translocase we used the series of DNA substrates depicted in Fig. 2a possessing a single 5′-$(dT)_L$ extension *L* (*L* = 15, 30, 45, 60, or 75 nts) and the results are shown in Fig. 2a. A burst of ATP hydrolysis is followed by a steady state rate of ATP hydrolysis. The burst phase amplitude increases with increasing ssDNA extension length, *L*, reflecting ATP hydrolysis during unwinding of the constant 24 bp duplex, and subsequent translocation of RecBC along the ssDNA extension of length, *L*. The steady-state phase of phosphate release after the burst phase reflects futile ATP hydrolysis by RecBC that remains bound to the end of the ssDNA extension as well as some small amount of rebinding of RecBC to the ssDNA due to incomplete trapping by heparin. These data were analyzed using Eq. (1) (parameters given in Table 1) and the slope of a plot of the burst phase amplitude as a function of the length of the $(dT)_L$ extension (Fig. 2a inset) indicates that the RecBC primary translocase consumes an average of 0.81 ± 0.05 ATP/nt translocated on these substrates.

ATP hydrolysis by RecBC during ssDNA translocation using only its secondary translocase

To examine the ATP coupling of RecBC while it uses only its secondary translocase activity we used the DNA substrates depicted in Fig. 2b possessing a single 3′-$(dT)_L$ extension L (L = 15, 30, 45, 60, or 75 nts) and the results are shown in Fig. 2b. Again, a burst of ATP hydrolysis is followed by a steady state phase for each DNA substrate, and the burst amplitude increases with increasing ssDNA extension length, L. These data were analyzed as described above (parameters given in Table 1) and indicate that the RecBC secondary translocase consumes an average of 1.12 ± 0.06 ATP/nt translocated on these substrates. We note that our previous studies [31] showed that after RecBC unwinds the 24 bp duplex of the DNA substrate depicted in Fig. 2b, the short unwound 5′-ended ssDNA remains bound in the primary RecB ssDNA binding site, thus continuing to activate the ATPase activity of RecB.

The differences between the amount of ATP hydrolyzed during RecBC translocation using only the primary translocase (0.81 ± 0.05 ATP/nt) vs. during RecBC translocation using only the secondary translocase (1.12 ± 0.06 ATP/nt) are slightly, but significantly different. This likely reflects the fact that the DNA substrates used for those two measurements are also different and thus the manner in which RecBC interacts with the two DNA substrates is also different. For example, on the single extension DNA substrate used to monitor 3′ to 5′ translocation, the canonical RecB motor can translocate unimpeded. However, on the single extension DNA substrate used to monitor 5′ to 3′ translocation, the canonical RecB motor remains bound to the short strand after duplex DNA unwinding,[31] otherwise the ATPase activity would not be stimulated by the ssDNA. Thus it is possible that this difference affects the resulting ATPase activities.

ATP hydrolysis by RecBC during ssDNA translocation using both its primary and secondary translocase activities

To examine the ATP coupling of RecBC while it translocates using both its primary and its secondary translocase activities we used the DNA substrates depicted in Fig. 3a possessing both a 5′-$(dT)_L$ extension L (L = 15, 30, 45, 60, or 75 nts) and a 3′-$(dT)_L$ extension (L = 15, 30, 45, 60, or 75 nts). For each DNA substrate, both ssDNA extensions were of the same length, L (with L = 15, 30, 45, 60, or 75 nts). These time courses are shown in Fig. 3a and were analyzed as described above (parameters given in Table 1). These results indicate that RecBC consumes an average of 1.07 ± 0.09 ATP/nt translocated on these double ssDNA extension substrates on which both the primary and secondary translocase activities can both operate simultaneously.[31] This value for the extent of ATP hydrolysis during RecBC translocation along the dual ssDNA extension substrates nearly encompasses the extremes of the estimates of ATP hydrolysis on the two single extension DNA substrates. Hence, we conclude that RecBC hydrolyzes one ATP to fuel translocation by one nucleotide irrespective of whether it moves along either strand independently or both strands simultaneously.

We have also determined the rate of RecBC translocation along the twin ssDNA extensions under these same low [ATP] conditions. Translocation experiments were performed as described [31] using the DNA substrate depicted in Fig. 3b. A lag phase is observed in the translocation time courses because RecBC must first unwind the 24 bp duplex and then translocate along the twin $(dT)_L$ ssDNA extensions before reaching the Cy3 fluorophore, whereupon the Cy3 fluorescence intensity increases, and then decreases upon RecBC dissociation from the DNA end. As observed previously [31], the duration of the lag phase increases linearly with increasing L, and the inverse of the slope of the plot of the lag time

versus *L* (Fig. 3b inset) indicates that RecBC translocates along the two ssDNA extensions with a rate of 238 ± 9 nt/s at 75 μM ATP.

A mutation within RecB slows both the primary and secondary rates of RecBC translocation

The results presented above indicate that within our uncertainties, RecBC hydrolyzes the same amount of ATP during ssDNA translocation using only the primary translocase, only the secondary translocase, or both translocases simultaneously. This suggests that both the primary and secondary translocase activities of RecBC are tightly coupled to the ATPase activity of the RecB motor. This predicts that a mutation within RecB that reduces the rate of its primary translocase activity should also reduce the rate of the secondary translocase activity within RecBC to the same extent if tight coupling is maintained. Amundsen et al. [41] have shown that mutation of Tyr803 to His (Y803H) within RecB slows the rate of unwinding of RecBCD. The Y803 residue resides within motif VI of RecB, a region that appears to be involved in coupling of ATP hydrolysis to DNA translocation in SF1 helicases.[41–43] We therefore introduced this mutation into RecB and examined whether it affects the rates of the primary and secondary RecBC translocases. We used the series of fluorescent DNA substrates depicted in Fig. 4 which have only a single $(dT)_L$ extension labeled with Cy3 at its end to independently monitor $RecB^{Y803H}C$ translocation in the 3′ to 5′ and 5′ to 3′ directions as described previously. [31] On these DNA substrates, RecBC initiates at the high affinity loading site (twin- $(dT)_6$ tailed fork) and upon addition of ATP, it unwinds the short duplex and then continues to translocate along the ssDNA extension until it reaches the Cy3 fluorophore resulting in an enhancement of Cy3 fluorescence. Hence, the assay measures the average time of arrival at the ssDNA end, as given by the lag time. By measuring the lag time as a function of varying the ssDNA extension length, *L*, one can estimate the rate of ssDNA translocation in either the 3′ to 5′ or 5′ to 3′ direction. The experiments shown in Fig. 4a and b were performed at 5 mM [ATP] (a higher [ATP] than used in the ATPase experiments above) and show that $RecB^{Y803H}C$ does translocate in the 3′ to 5′ direction, with a much slower average rate of 215 ± 11 nt/s (Fig. 4a) (compared to wtRecBC). Furthermore, the data in Fig. 4b show that $RecB^{Y803H}C$ also translocates in the 5′ to 3′ direction, with a similarly slower rate of 248 ± 20 nt/s. For comparison, Fig. 4c and 4d show that the translocation rates for wild type RecBC also at 5 mM ATP are much faster than for $RecB^{Y80H}C$ for both the primary (3′ to 5: 947 ± 51 nt/s) and secondary (5′ to 3: 1160 ± 77 nt/s) translocases on this same series of substrates under the same conditions [31]. Therefore, the $RecB^{Y803H}$ mutation slows both the primary and secondary translocase rates within $RecB^{Y803H}C$. Fig. 4e (see also supplementary Fig. 2) shows that both the primary and secondary translocase rates for $RecB^{Y803H}C$ decrease with decreasing [ATP] with similar K_M values, but much higher than observed for wild type RecBC [31], indicating that both primary and secondary translocase activities are driven by the RecB ATPase site. We note that using these two single extension DNA substrates, we observe that the 5′ to 3′ rates are slightly faster than the 3′ to 5′ rates. This may reflect that the DNA substrates are not identical and for the substrates in Fig. 4b, RecB remains bound to the end of the shorter DNA after the duplex is unwound.[31] A similar small rate difference was also observed in experiments with wt RecBC (see Fig. 4c and d and reference [31]) using these same substrates, whereas the primary and secondary rates were found to be identical on double ssDNA extension DNA substrates.[31] We note the slight difference in the primary and secondary rates also correlates with a slight difference in the extent of ATP hydrolysis by RecBC when it translocates using only its primary translocase (0.81 ± 0.05 ATP/nt), vs. only its secondary translocase (1.12 ± 0.06 ATP/nt). Even so, these data show that a single mutation within RecB slows down both the primary and secondary RecBC translocase activities to the same extent, consistent with our conclusion that the RecB ATPase activity drives both translocases in a highly coupled reaction.

ATP coupling stoichiometry during DNA unwinding by RecBC

We also measured the extent of ATP hydrolysis by RecBC during DNA unwinding (bp melting plus ssDNA translocation) to compare with the ATP hydrolysis measured for only ssDNA translocation without DNA unwinding in Fig. 3a. The series of DNA substrates used in these studies possess a high affinity RecBC loading site (5′-$(dT)_6$, 3′-$(dT)_6$ ssDNA tails) at one end of a duplex region of variable length *L* followed by a constant 40 nucleotide 3′ ssDNA as depicted in Fig. 5a. Although RecBC will continue to translocate along the 40 nt ssDNA extension after it unwinds the DNA duplex, this will contribute a constant amount of ATP hydrolysis since each DNA substrate contains the same $(dT)_{40}$ ssDNA extension. Hence, the slope of a plot of ATP hydrolyzed versus duplex length will yield the ATP consumption per bp unwound by RecBC.

When RecBC unwinds the DNA, there is a burst of phosphate released followed by a slower steady-state release of phosphate. The burst phase reflects the amount of ATP consumed during the unwinding of the duplex of length *L* (*L* = 24, 29, 37, 40, 43, 48, 53, and 60 bp) as well as during the translocation of RecBC along the 40 nt ssDNA extension. The time courses in Fig. 5a were analyzed using Eq. (1) and the resulting parameters are summarized in Table 1. The burst phase amplitudes are plotted versus the corresponding duplex length (Fig. 5a inset), yielding an average of 0.96 ± 0.08 ATP/bp unwound during RecBC catalyzed DNA unwinding. Fig. 5b shows unwinding time courses at the same [ATP] used to measure ATP hydrolysis. These unwinding time courses were analyzed as described previously [27] yielding a DNA unwinding rate of 114 ± 4 bp/s. Therefore, under the same conditions, the rate of DNA unwinding by RecBC is only a factor of 2 lower than the rate of ssDNA translocation using both its primary and secondary translocase activities in the absence of DNA unwinding (238 ± 9 nt/s Fig. 3b).

Discussion

The RecB ATPase activity drives both the primary and secondary translocase activities within RecBC

We recently discovered that RecBC possesses two translocase activities, both driven by the single RecB ATPase motor.[31] We refer to the canonical (3′ to 5′) translocase activity as the primary translocase since it moves along ssDNA in the same direction as the RecB monomeric motor. The other novel translocase activity is referred to as the secondary translocase. When two ssDNA extensions are available, RecBC uses both translocase activities to move along both strands at the same rate, even in the absence of DNA unwinding. Interestingly, this secondary translocase activity is insensitive to the backbone polarity of the ssDNA,[31] hence it is possible that it actually reflects a double stranded translocase activity that normally operates during DNA unwinding, although our assay detects it as a ssDNA translocase activity. Although we have not yet identified the region of RecBC that is responsible for this secondary translocase activity, there are two likely possibilities. It may reside within the arm region of the RecB subunit that is seen to interact with the duplex region in the RecBCD-DNA crystal structure and/or within the dead nuclease domain within RecC that interacts with the 5′ ssDNA of the DNA fork.

If the single ATPase site within the RecB motor drives conformational changes within RecBC that control both the primary and secondary translocase activities to move at the same rates, this predicts that the amount of ATP hydrolyzed per nucleotide translocated should be the same or nearly the same whether one or both translocases are operational. In fact, this is what we observe in the experiments reported here. We measure 1.0 ± 0.15 ATP hydrolyzed per nucleotide translocated regardless of whether RecBC translocates using only its primary translocase, only its secondary translocase or both simultaneously. This supports

the view that the ATP-induced RecBC conformational changes that drive both translocase activities and are tightly coupled. Of course, such coupled long range motions in proteins are the basis for much of allostery.[45] The novel aspect of our results is that conformational changes affected by ATP hydrolysis by the canonical RecB motor appear to be tightly coupled to and drive a second translocation activity at a distant site within RecBC. This indicates the importance of considering the properties of the entire molecular machine for RecBC or RecBCD, and likely for other machines that move along nucleic acids.

ATP coupling during DNA unwinding vs. ssDNA translocation

Interestingly, we show that the amount of ATP hydrolyzed during processive DNA unwinding (bp melting plus translocation) by RecBC (0.96 ± 0.08 ATP/bp unwound) is the same as during ssDNA translocation along both DNA strands without DNA unwinding (1.07 ± 0.09 ATP/nt) indicating that no additional ATP is required for RecBC to unwind and translocate than to only translocate along ssDNA. This result is consistent with previous estimates for ATP consumption during DNA unwinding by RecBCD (~ 2–3 ATP/bp unwound) and by RecBC during DNA unwinding (~ 1.2–1.4 ATP/bp).[46] This suggests that most, if not all, of the energy obtained from ATP binding and hydrolysis is used to fuel RecBC translocation. Furthermore, the rate of unwinding is reduced only by ~two-fold compared to the rate of ssDNA translocation using both the primary and secondary translocase activities, suggesting that DNA unwinding by RecBC occurs by an active mechanism.[48–51]

The results reported here are consistent with two models for the mechanism of DNA unwinding by RecBC. Based on the fact that RecBCD [28] as well as RecBC [30] can melt out 5–6 bp upon binding to a duplex DNA end in an ATP-independent reaction, it is possible that DNA melting occurs in 4–6 bp steps in an ATP-independent reaction, and that ATP hydrolysis is used solely to translocate RecBC along the newly unwound ssDNA. When translocation brings RecBC to the ss-ds DNA junction, then the enzyme is reset and ATP-independent melting of 4–6 bp is repeated, etc. This model is also supported by the observation of a 4 bp kinetic step size for DNA unwinding by both RecBC [27] and RecBCD. [52] In the second model, DNA melting and ssDNA translocation occur simultaneously, one bp at a time.[6] Differentiation between these two models will require the direct measurement of the DNA unwinding step size in a single molecule experiment.

Materials and Methods

Buffers and Reagents

All buffers were prepared with reagent grade chemicals and doubly-distilled water that was deionized further using a Milli-Q purification system (Millipore Corp., Bedford, MA). Solutions were filtered through 0.2 micron filters after preparation. Buffer M is 20 mM Mops-KOH (pH 7.0 at 25°C), 30 mM NaCl, 10 mM $MgCl_2$, 1 mM 2-ME, 5% (v/v) glycerol. Heparin stock solution was prepared by dissolving heparin sodium salt (Sigma, St. Louis, MO) in Buffer M and dialyzing the mixture extensively against Buffer M using 3500 molecular weight cut-off dialysis tubing. Heparin stock solution was stored at 4°C until use and its concentration was determined by titration with Azure A as described.[37] ATP stock solution was prepared as described previously and stored at −20°C until use.[27]

Proteins

E. coli RecB, $RecB^{Y803H}$ and RecC were purified separately and stored at −80°C as described. [53] The RecBC and $RecB^{Y803H}C$ heterodimers were reconstituted by mixing equal molar ratios of RecB or $RecB^{Y803H}$ and RecC on ice. RecBC and $RecB^{Y803H}C$ were dialyzed against Buffer M at 4°C before use and the concentrations determined

spectrophotometrically using an extinction coefficient of $\varepsilon_{280} = 3.9\times10^5\ M^{-1}cm^{-1}$.[27] *E. coli* phosphate binding protein (PBP) was purified, labeled with coumarin (MDCC) (Invitrogen, Carlsbad, CA), and stored at −80°C until use as described.[37]

DNA

Oligodeoxynucleotides, either unlabeled or labeled covalently with Cy3 or Cy5, were synthesized, purified, and their concentrations were determined as described.[27] DNA stock solutions were stored at −20°C until use. The sequences of the DNA substrates are given in Supplementary Table 1 and 2.

Stopped-flow fluorescence experiments

All stopped-flow fluorescence measurements were collected using an SX.18MV stopped-flow apparatus (Applied Photophysics Ltd., Leatherhead, UK). All experiments, except those in Fig. 4, were performed in Buffer M at 25°C. The translocation experiments performed with $RecB^{Y803H}C$ and wtRecBC (Fig. 4) were performed in Buffer M containing 250mM NaCl at 25°C. This higher [NaCl] increased the Cy3 fluorescence signal compared to data obtained at 30 mM NaCl as shown previously for wtRecBC.[31] However, the rates of translocation are unaffected by the change in [NaCl].

Phosphate release experiments were performed as described previously.[37] DNA substrate (200 nM) was equilibrated with RecBC (20 nM) in one syringe of the instrument and the reaction was initiated by 1:1 mixing with ATP (150 μM), heparin (10 mg/mL), and PBP-MDCC (40 μM). Final conditions are therefore: 100 nM DNA, 10 nM RecBC, 75 μM ATP, 5 mg/mL heparin, and 20 μM PBP-MDCC in Buffer M. Identical experiments were performed without the DNA substrate to access the amount of phosphate contamination in buffers and reagents and also any background hydrolysis that may occur with RecBC. PBP-MDCC fluorescence was excited at 430 nm and its emission was collected at all wavelengths > 450 nm using a cutoff filter (Oriel Corp., Stratford, CT).

PBP-MDCC was calibrated by mixing the same ATP solution used in phosphate release experiments (150 μM ATP, 10 mg/mL heparin, and 40 μM PBP-MDCC) with various phosphate standards of 0, 0.5, 1.0, 1.5, 2.0, 2.5, 3.0, and 5 μM as described previously [37].

DNA translocation experiments were performed by incubating single extension $(dT)_L$ DNA substrates (200 nM) (L = 15, 30, 45, 60, 75) with wtRecBC or $RecB^{Y803H}C$ (150 nM) in one syringe of the apparatus and DNA translocation was initiated by 1:1 mixing with ATP (final concentration: 0.5 mM, 1 mM, 2mM, 5 mM, and 8 mM) and heparin (15 mg/mL) as described.[31] Cy3 fluorescence was excited at 515 nm and its emission was collected using >570 nm cut-off filter (Oriel Corp., Stratford, CT).

DNA unwinding experiments were performed by incubating DNA substrate (40 nM) (L = 24, 29, 37, 40, 43, 48, 53, and 60 bp) with RecBC (200 nM) in one syringe of the apparatus and DNA unwinding was initiated by 1:1 mixing with ATP (20 μM, 75 μM, 150 μM, 240 μM, 832 μM, 2.8 mM, and 10 mM) and heparin (15 mg/mL) as described.[27] Cy5 fluorescence was excited at 515 nm and its emission was collected at 570 nm using an interference filter (Oriel Corp., Stratford, CT) while Cy5 fluorescence was monitored simultaneously at all wavelengths > 665 nm using a cutoff filter (Oriel Corp., Stratford, CT).

Analysis of phosphate release kinetics

In order to determine the amount of phosphate released from the fluorescence signal obtained from phosphate release time courses, a calibration experiment was performed as described above by mixing the ATP, heparin, and PBP-MDCC solution with known

concentrations of phosphate standard. These resulting traces were fit to a single exponential function ($Ae^{-kx} + C$) and the plateau value, C, was plotted versus phosphate standard concentration to obtain a calibration curve (Supplementary Fig. 1). The fluorescence values from the phosphate release experiments fall within the linear region of the calibration curve and these time courses were analyzed using Eq. (1) which describes a burst of phosphate released followed by a steady-state phase of phosphate released.

$$Pi(t)=A_b(1-e^{-k_b t})+k_{ss}t \quad (1)$$

As can be seen from Table 1, both the burst amplitude, A_b, and the steady state ATPase rates, k_{ss}, increase with increasing length for all experiments. The increase in A_b with DNA length reflects the increase in ATP hydrolysis during unwinding and/or translocation along the longer DNA. The small increase in k_{ss} reflects a small amount of rebinding of dissociated RecBC to the single stranded DNA (after it has completed unwinding and ssDNA translocation) due to incomplete trapping by heparin. It also may reflect a slower rate of dissociation of RecBC from the longer DNA. We observed the same phenomenon, although to a lesser extent in our UvrD studies [37]. However, this does not affect the amplitude of the burst phase, A_b, obtained from the fitting to Eq. (1) since the burst phase is due to RecBC that is initially bound to the high affinity loading site and all of the RecBC is initially bound to the high affinity loading site at the start of the experiment. Furthermore, Eq. (1) corrects for any small contributions of the steady state phase to the burst amplitude.

Analysis of DNA unwinding time courses

Global NLLS analysis of DNA unwinding time courses was performed using Conlin (provided by Dr. Jeremy Williams and modified by Dr. Aaron Lucius) and IMSL C Numerical Libraries (Visual Numeric Incorporated, Houston, TX) as described previously [27]. The uncertainties reported reflect 68% confidence interval limits determined from a 50 cycle Monte Carlo analysis as described [52–55]. Unwinding time courses were fit to Eq. (2) based on mechanism shown in Scheme 1, by obtaining the time-dependent formation of ssDNA, $f_{ss}(t)$, as the inverse Laplace transform of $F_{ss}(s)$ using numerical methods as described [27]. For Scheme 1, $f_{ss}(t)$ is given by Eq. (2):

$$\begin{aligned} f_{ss}(t) &= A_T \mathscr{L}^{-1} F_{ss}(s) \\ &= A_T \mathscr{L}^{-1} \left(\frac{k_{obs}^n (k_{NP}+sx)}{s(k_{NP}+s)(k_{obs}+s)^n} \right) \end{aligned} \quad (2)$$

where $F_{ss}(s)$ is the Laplace transform of $f_{ss}(t)$, L^{-1} is the inverse Laplace transform operator with s as the Laplace variable, A_T is the total amplitude for a given duplex length L, n is the number of unwinding steps with k_{obs} being the rate constant in between two successive unwinding steps, k_{NP} is the isomerization rate constant for the conversion of non-productive, $(RD)_{NP}$, to productive, $(RD)_L$, RecBC-DNA complexes, and x is the fraction of productively bound RecBC-DNA complexes. The average kinetic step-size, m, can be determined by NLLS analysis by replacing n in Eq. (2) with L/m. Alternatively, m can be determined from the slope of a plot of n vs L.

Analysis of DNA translocation time courses

Rates of ssDNA translocation were obtained as described [31] from analysis of multiple translocation experiments performed as a function of ssDNA extension length, L and determining the inverse of the slope of a plot of lag time vs. ssDNA extension length. A plot of the macroscopic translocation rate (V_{trans}) versus [ATP] was fit to Eq. (3) to obtain K_M and V_{max}.

$$V_{trans} = \frac{V_{max}[ATP]}{K_M + [ATP]} \quad (3)$$

Supplementary Material

Refer to Web version on PubMed Central for supplementary material.

Acknowledgments

This research was supported in part by NIH grant GM045948. We thank Thang Ho for synthesis and purification of DNA, Dr. Elizabeth Weiland for making the overexpression plasmid for RecB^{Y803H}, Josh Brettmann for preliminary studies of RecB^{Y803H}C, Drs. C. Fischer, A. Lucius, and E. Tomko for discussions of data analysis and Drs. G. Smith and D. Julin for providing plasmids and cell lines.

References

1. Delagoutte E, von Hippel PH. Helicase mechanisms and the coupling of helicases within macromolecular machines. Part I: Structures and properties of isolated helicases. Q Rev Biophys. 2002; 35:431–78. [PubMed: 12621862]
2. Lohman TM, Tomko EJ, Wu CG. Non-hexameric DNA helicases and translocases: mechanisms and regulation. Nat Rev Mol Cell Biol. 2008; 9:391–401. [PubMed: 18414490]
3. Matson SW, Bean DW, George JW. DNA helicases: enzymes with essential roles in all aspects of DNA metabolism. Bioessays. 1994; 16:13–22. [PubMed: 8141804]
4. Patel SS, Picha KM. Structure and function of hexameric helicases. Annu Rev Biochem. 2000; 69:651–97. [PubMed: 10966472]
5. Lohman TM, Bjornson KP. Mechanisms of helicase-catalyzed DNA unwinding. Annu Rev Biochem. 1996; 65:169–214. [PubMed: 8811178]
6. Singleton MR, Dillingham MS, Wigley DB. Structure and mechanism of helicases and nucleic acid translocases. Annu Rev Biochem. 2007; 76:23–50. [PubMed: 17506634]
7. Anderson DG, Kowalczykowski SC. The translocating RecBCD enzyme stimulates recombination by directing RecA protein onto ssDNA in a chi-regulated manner. Cell. 1997; 90:77–86. [PubMed: 9230304]
8. Kowalczykowski SC, Dixon DA, Eggleston AK, Lauder SD, Rehrauer WM. Biochemistry of homologous recombination in Escherichia coli. Microbiol Rev. 1994; 58:401–65. [PubMed: 7968921]
9. Smith GR. Homologous recombination in prokaryotes: enzymes and controlling sites. Genome. 1989; 31:520–7. [PubMed: 2534386]
10. Dillingham MS, Kowalczykowski SC. RecBCD enzyme and the repair of double-stranded DNA breaks. Microbiol Mol Biol Rev. 2008; 72:642–71. Table of Contents. [PubMed: 19052323]
11. Dillingham MS, Spies M, Kowalczykowski SC. RecBCD enzyme is a bipolar DNA helicase. Nature. 2003; 423:893–7. [PubMed: 12815438]
12. Finch PW, Storey A, Brown K, Hickson ID, Emmerson PT. Complete nucleotide sequence of recD, the structural gene for the alpha subunit of Exonuclease V of Escherichia coli. Nucleic Acids Res. 1986; 14:8583–94. [PubMed: 3537961]
13. Finch PW, Storey A, Chapman KE, Brown K, Hickson ID, Emmerson PT. Complete nucleotide sequence of the Escherichia coli recB gene. Nucleic Acids Res. 1986; 14:8573–82. [PubMed: 3537960]
14. Taylor AF, Smith GR. RecBCD enzyme is a DNA helicase with fast and slow motors of opposite polarity. Nature. 2003; 423:889–93. [PubMed: 12815437]
15. Rigden DJ. An inactivated nuclease-like domain in RecC with novel function: implications for evolution. BMC Struct Biol. 2005; 5:9. [PubMed: 15985153]

16. Spies M, Amitani I, Baskin RJ, Kowalczykowski SC. RecBCD enzyme switches lead motor subunits in response to chi recognition. Cell. 2007; 131:694–705. [PubMed: 18022364]
17. Yu M, Souaya J, Julin DA. Identification of the nuclease active site in the multifunctional RecBCD enzyme by creation of a chimeric enzyme. J Mol Biol. 1998; 283:797–808. [PubMed: 9790841]
18. Yu M, Souaya J, Julin DA. The 30-kDa C-terminal domain of the RecB protein is critical for the nuclease activity, but not the helicase activity, of the RecBCD enzyme from Escherichia coli. Proc Natl Acad Sci USA. 1998; 95:981–6. [PubMed: 9448271]
19. Anderson DG, Churchill JJ, Kowalczykowski SC. Chi-activated RecBCD enzyme possesses 5′-->3′ nucleolytic activity, but RecBC enzyme does not: evidence suggesting that the alteration induced by Chi is not simply ejection of the RecD subunit. Genes Cells. 1997; 2:117–28. [PubMed: 9167969]
20. Handa N, Bianco PR, Baskin RJ, Kowalczykowski SC. Direct visualization of RecBCD movement reveals cotranslocation of the RecD motor after chi recognition. Mol Cell. 2005; 17:745–50. [PubMed: 15749023]
21. Arnold DA, Kowalczykowski SC. Facilitated loading of RecA protein is essential to recombination by RecBCD enzyme. J Biol Chem. 2000; 275:12261–5. [PubMed: 10766864]
22. Spies M, Bianco PR, Dillingham MS, Handa N, Baskin RJ, Kowalczykowski SC. A molecular throttle: the recombination hotspot chi controls DNA translocation by the RecBCD helicase. Cell. 2003; 114:647–54. [PubMed: 13678587]
23. Spies M, Dillingham MS, Kowalczykowski SC. Translocation by the RecB motor is an absolute requirement for {chi}-recognition and RecA protein loading by RecBCD enzyme. J Biol Chem. 2005; 280:37078–87. [PubMed: 16041060]
24. Smith GR. How RecBCD Enzyme and Chi Promote DNA Break Repair and Recombination: a Molecular Biologist's View. Microbiol Mol Biol Rev. 2012; 76:217–28. [PubMed: 22688812]
25. Bianco PR, Kowalczykowski SC. Translocation step size and mechanism of the RecBC DNA helicase. Nature. 2000; 405:368–72. [PubMed: 10830968]
26. Korangy F, Julin DA. Kinetics and processivity of ATP hydrolysis and DNA unwinding by the RecBC enzyme from Escherichia coli. Biochemistry. 1993; 32:4873–80. [PubMed: 8387820]
27. Wu CG, Lohman TM. Influence of DNA end structure on the mechanism of initiation of DNA unwinding by the Escherichia coli RecBCD and RecBC helicases. J Mol Biol. 2008; 382:312–26. [PubMed: 18656489]
28. Farah JA, Smith GR. The RecBCD enzyme initiation complex for DNA unwinding: enzyme positioning and DNA opening. J Mol Biol. 1997; 272:699–715. [PubMed: 9368652]
29. Singleton MR, Dillingham MS, Gaudier M, Kowalczykowski SC, Wigley DB. Crystal structure of RecBCD enzyme reveals a machine for processing DNA breaks. Nature. 2004; 432:187–93. [PubMed: 15538360]
30. Wong CJ, Lohman TM. Kinetic control of Mg2+-dependent melting of duplex DNA ends by Escherichia coli RecBC. J Mol Biol. 2008; 378:761–77. [PubMed: 18395743]
31. Wu CG, Bradford C, Lohman TM. Escherichia coli RecBC helicase has two translocase activities controlled by a single ATPase motor. Nat Struct Mol Biol. 2010; 17:1210–7. [PubMed: 20852646]
32. Wong CJ, Lucius AL, Lohman TM. Energetics of DNA end binding by E. coli RecBC and RecBCD helicases indicate loop formation in the 3′-single-stranded DNA tail. J Mol Biol. 2005; 352:765–82. [PubMed: 16126227]
33. Wong CJ, Rice RL, Baker NA, Ju T, Lohman TM. Probing 3′-ssDNA loop formation in E. coli RecBCD/RecBC-DNA complexes using non-natural DNA: a model for "Chi" recognition complexes. J Mol Biol. 2006; 362:26–43. [PubMed: 16901504]
34. Brune M, Hunter JL, Howell SA, Martin SR, Hazlett TL, Corrie JE, Webb MR. Mechanism of inorganic phosphate interaction with phosphate binding protein from Escherichia coli. Biochemistry. 1998; 37:10370–80. [PubMed: 9671505]
35. Dillingham MS, Wigley DB, Webb MR. Demonstration of unidirectional single-stranded DNA translocation by PcrA helicase: measurement of step size and translocation speed. Biochemistry. 2000; 39:205–12. [PubMed: 10625495]

36. Dillingham MS, Wigley DB, Webb MR. Direct measurement of single-stranded DNA translocation by PcrA helicase using the fluorescent base analogue 2-aminopurine. Biochemistry. 2002; 41:643–51. [PubMed: 11781105]
37. Tomko EJ, Fischer CJ, Niedziela-Majka A, Lohman TM. A nonuniform stepping mechanism for E. coli UvrD monomer translocation along single-stranded DNA. Mol Cell. 2007; 26:335–47. [PubMed: 17499041]
38. Slatter AF, Thomas CD, Webb MR. PcrA helicase tightly couples ATP hydrolysis to unwinding double-stranded DNA, modulated by the initiator protein for plasmid replication, RepD. Biochemistry. 2009; 48:6326–34. [PubMed: 19473041]
39. Toseland CP, Martinez-Senac MM, Slatter AF, Webb MR. The ATPase cycle of PcrA helicase and its coupling to translocation on DNA. J Mol Biol. 2009; 392:1020–32. [PubMed: 19647000]
40. Kim DE, Narayan M, Patel SS. T7 DNA helicase: a molecular motor that processively and unidirectionally translocates along single-stranded DNA. J Mol Biol. 2002; 321:807–19. [PubMed: 12206763]
41. Amundsen SK, Taylor AF, Reddy M, Smith GR. Intersubunit signaling in RecBCD enzyme, a complex protein machine regulated by Chi hot spots. Genes Dev. 2007; 21:3296–307. [PubMed: 18079176]
42. Graves-Woodward KL, Gottlieb J, Challberg MD, Weller SK. Biochemical analyses of mutations in the HSV-1 helicase-primase that alter ATP hydrolysis, DNA unwinding, and coupling between hydrolysis and unwinding. J Biol Chem. 1997; 272:4623–30. [PubMed: 9020191]
43. Hall MC, Ozsoy AZ, Matson SW. Site-directed mutations in motif VI of Escherichia coli DNA helicase II result in multiple biochemical defects: evidence for the involvement of motif VI in the coupling of ATPase and DNA binding activities via conformational changes. J Mol Biol. 1998; 277:257–71. [PubMed: 9514760]
44. Saikrishnan K, Griffiths SP, Cook N, Court R, Wigley DB. DNA binding to RecD: role of the 1B domain in SF1B helicase activity. EMBO J. 2008; 27:2222–9. [PubMed: 18668125]
45. Goodey NM, Benkovic SJ. Allosteric regulation and catalysis emerge via a common route. Nat Chem Biol. 2008; 4:474–82. [PubMed: 18641628]
46. Korangy F, Julin DA. Efficiency of ATP hydrolysis and DNA unwinding by the RecBC enzyme from Escherichia coli. Biochemistry. 1994; 33:9552–60. [PubMed: 8068630]
47. Roman LJ, Kowalczykowski SC. Characterization of the helicase activity of the Escherichia coli RecBCD enzyme using a novel helicase assay. Biochemistry. 1989; 28:2863–73. [PubMed: 2545238]
48. Lohman TM. Helicase-catalyzed DNA unwinding. J Biol Chem. 1993; 268:2269–72. [PubMed: 8381400]
49. Betterton MD, Julicher F. Opening of nucleic-acid double strands by helicases: active versus passive opening. Phys Rev E Stat Nonlin Soft Matter Phys. 2005; 71:011904. [PubMed: 15697627]
50. Manosas M, Xi XG, Bensimon D, Croquette V. Active and passive mechanisms of helicases. Nucleic Acids Res. 2010; 38:5518–26. [PubMed: 20423906]
51. Lohman TM. Escherichia coli DNA helicases: mechanisms of DNA unwinding. Mol Microbiol. 1992; 6:5–14. [PubMed: 1310794]
52. Lucius AL, Vindigni A, Gregorian R, Ali JA, Taylor AF, Smith GR, Lohman TM. DNA unwinding step-size of E. coli RecBCD helicase determined from single turnover chemical quenched-flow kinetic studies. J Mol Biol. 2002; 324:409–28. [PubMed: 12445778]
53. Lucius AL, Wong CJ, Lohman TM. Fluorescence stopped-flow studies of single turnover kinetics of E. coli RecBCD helicase-catalyzed DNA unwinding. J Mol Biol. 2004; 339:731–50. [PubMed: 15165847]
54. Fischer CJ, Maluf NK, Lohman TM. Mechanism of ATP-dependent translocation of E. coli UvrD monomers along single-stranded DNA. J Mol Biol. 2004; 344:1287–309. [PubMed: 15561144]
55. Fischer CJ, Lohman TM. ATP-dependent translocation of proteins along single-stranded DNA: models and methods of analysis of pre-steady state kinetics. J Mol Biol. 2004; 344:1265–86. [PubMed: 15561143]

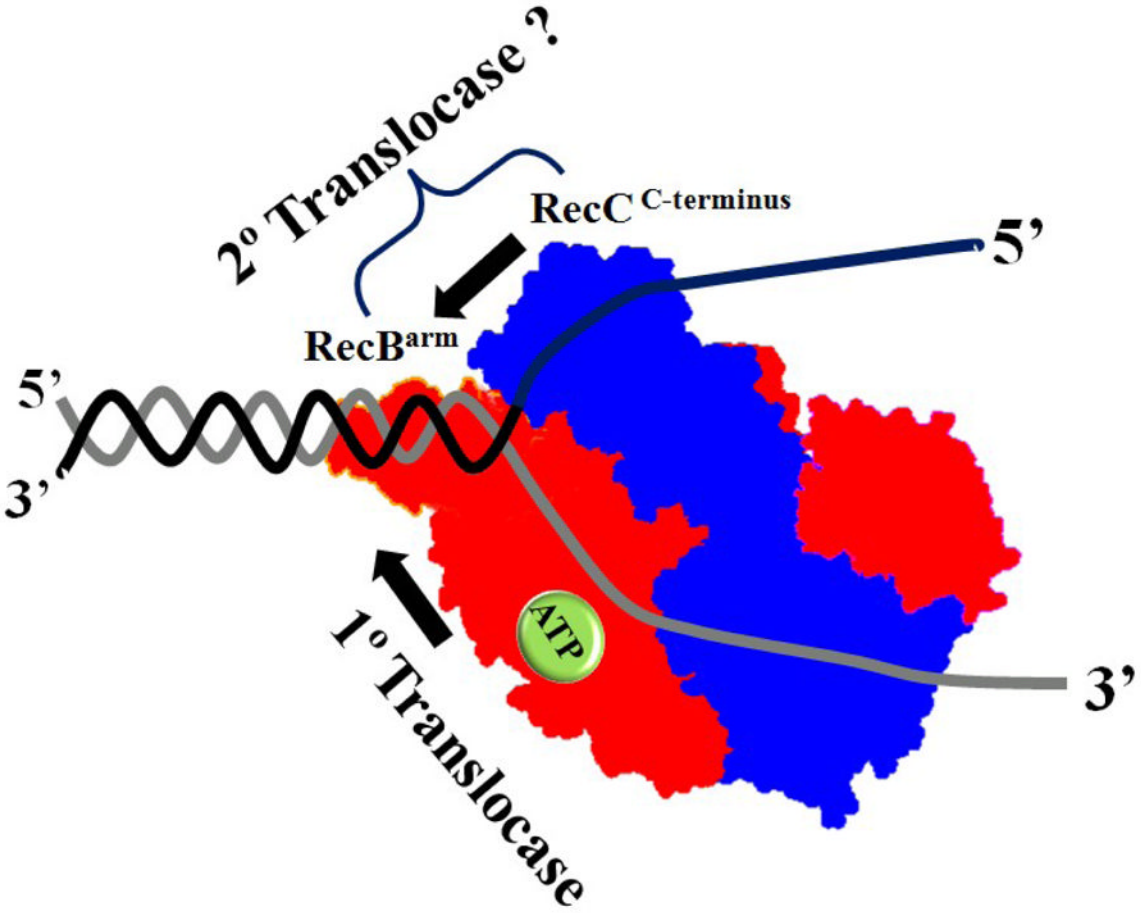

Fig. 1.

Schematic of a RecBC-DNA structure. The pathways of the single stranded DNA, the position of the RecB ATPase site, the position of the primary RecBC translocase and the putative position of the secondary RecBC translocase are shown along with the RecB and RecC subunits.

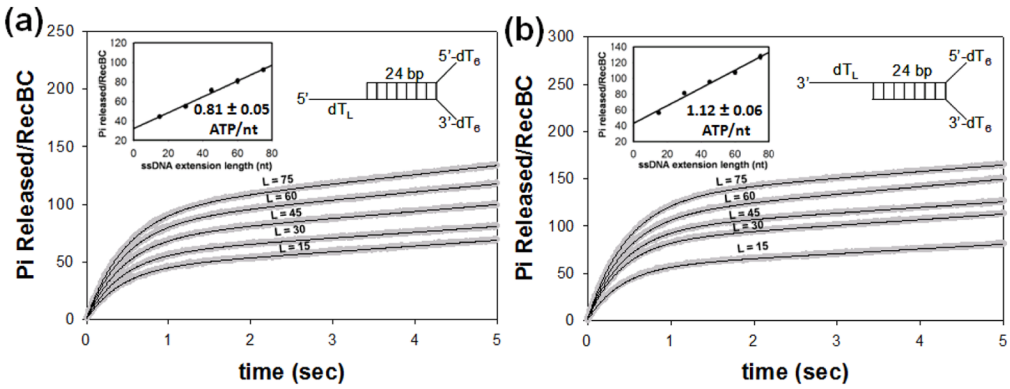

Fig 2.

ATP coupling stoichiometry during ssDNA translocation by RecBC using its primary or secondary translocases. (a). Time courses of phosphate release during RecBC unwinding of a short (24 bp) duplex and subsequent translocation using its primary translocase activity along a series of ssDNA extensions (depicted schematically and in panel a). The smooth curves are simulations based on the best fit parameters (see Table 1) determined from fits of each time course to Eq. (1). (a inset)-Plot of the burst phase amplitude as a function of ssDNA extension length. A linear fit to the data ($[P_i] = 0.8132L + 32.16$), yields an average of 0.81±0.05 ATP/nucleotide translocated for the primary RecBC ssDNA translocase (in the absence of DNA unwinding). (b). Time courses of phosphate release during RecBC unwinding of a short (24 bp) duplex and subsequent translocation using its secondary translocase activity along the series of ssDNA extensions depicted. The smooth curves are simulations based on the best fit parameters (see Table 1) determined from fits of each time course to Eq. (1). (b inset)- Plot of the burst phase amplitude as a function of ssDNA extension length. A linear fit to the data ($[P_i] = 1.1223L + 43.14$), yields an average of 1.12±0.06 ATP/nucleotide translocated for the secondary RecBC ssDNA translocase.

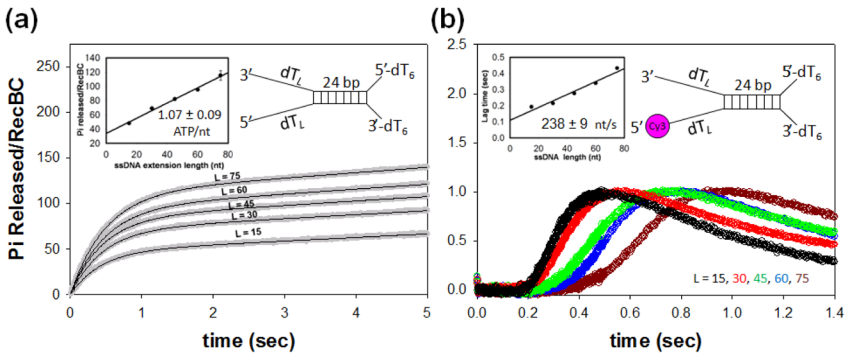

Fig. 3.

ATP coupling stoichiometry during RecBC translocation using both primary and secondary translocase activities simultaneously. (a). Time courses of phosphate release during RecBC unwinding of a short (24 bp) duplex and subsequent translocation using both translocase activities along the series of twin ssDNA extensions depicted. The smooth curves are simulations based on the best fit parameters (see Table 1) determined from fits of each time course to Eq. (1). (a inset)- Plot of the burst phase amplitude as a function of ssDNA extension length. The line is a linear fit to the data ($[P_i] = 1.0696L + 33.76$), yielding an average of 1.07±0.09 ATP/"bp" for simultaneous translocation of RecBC along both ssDNA extensions (in the absence of DNA unwinding). (b)-RecBC translocation time courses under the same solution conditions and 75 μM ATP. (b inset)- lag time analysis results in a translocation rate of 238±9 nt/s (lag time = $0.004L + 0.1092$).

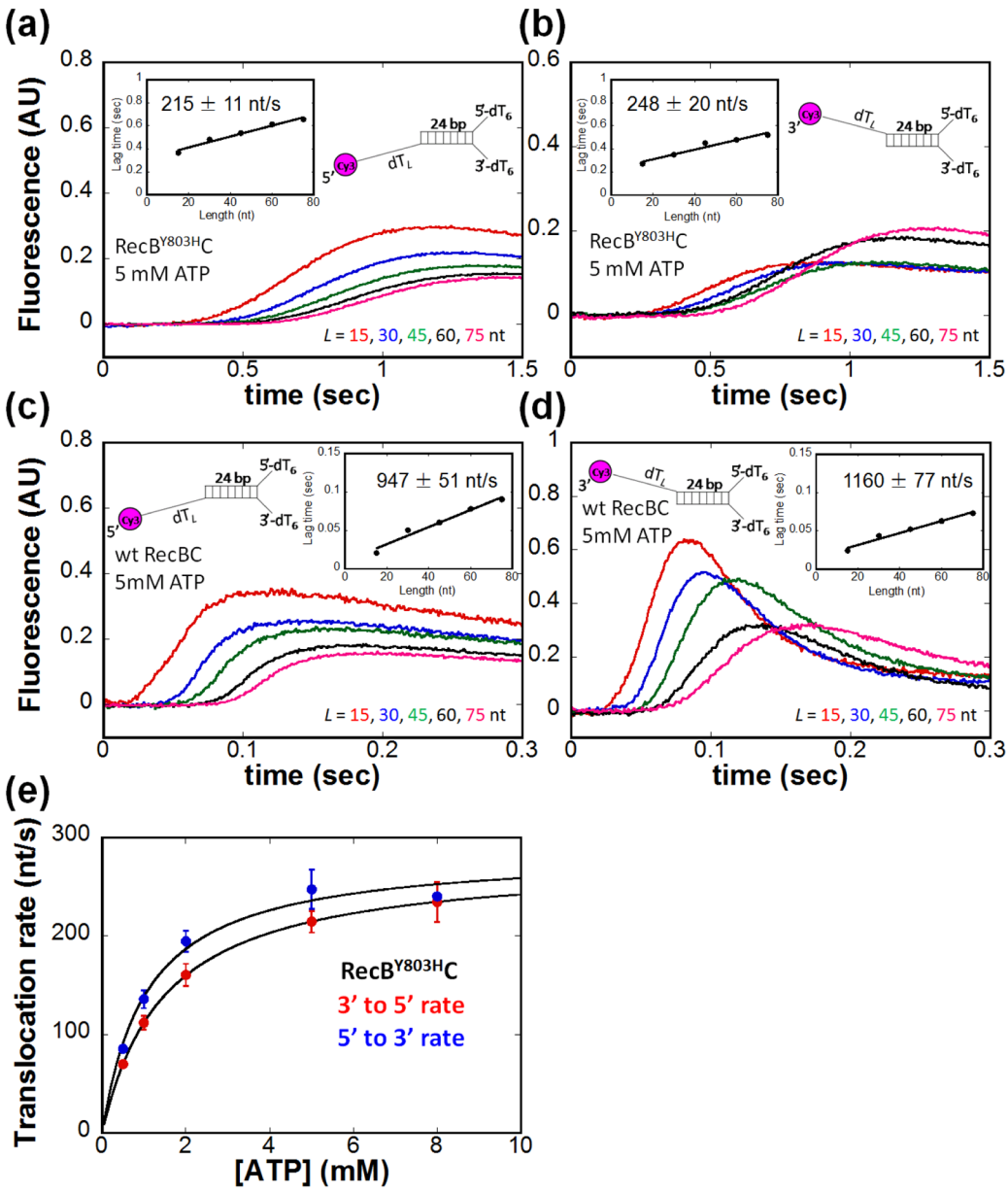

Fig. 4.

The rates of the primary and secondary translocases are both reduced in RecB^{Y803H}C compared with wtRecBC. (a). Translocation time courses for the RecB^{Y803H}C primary translocase in the 3′ to 5′ direction using a series of 5′-Cy3 labeled single extension DNA substrates. (a inset)- Plots of the lag time vs. the ssDNA extension length, *L*. The inverse of the slope yields an average 3′ to 5′ rate of 215 ± 11 nt/s (three sets of experiments). (b)- Translocation time courses for the RecB^{Y803H}C secondary translocase in the 5′ to 3′ direction using a series of 3′-Cy3 labeled single extension DNA substrates. (b inset)- Plots of the lag time vs. the ssDNA extension length, *L*. The inverse of the slope yields an average 5′ to 3′ rate of 248±20 nt/s (three sets of experiments). (c)- Translocation time courses for the wtRecBC primary translocase. (c inset)- Plots of the lag time vs. the ssDNA extension length, *L*. The inverse of the slope of yields an average 3′ to 5′ rate of 947 ± 51 nt/s (five sets of experiments). (d)-Translocation time courses for the wtRecBC secondary translocase. (d

inset)- Plots of the lag time vs. the ssDNA extension length, *L*. The inverse of the slope yields an average 5′ to 3′rate of 1160 ± 77 nt/s (five sets of experiments). (e)- Dependence on [ATP] of the 3′ to 5′ translocation rates (red circles) (K_M=1.47±0.01 mM; V_{max}=278±50 nt/s) and the 5′ to 3′ translocation rate (blue circles) (K_M=1.06±0.18 mM; V_{max}=286±14 nt/s) for $RecB^{Y803H}C$. Curves are fits to the Michaelis-Menten equation Eq. (3).

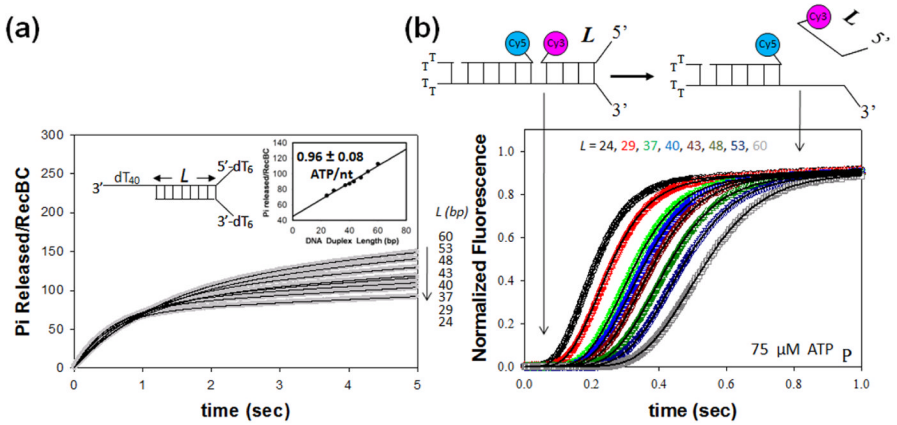

Fig. 5.

ATP coupling stoichiometry during DNA unwinding by RecBC. (a). Time courses of phosphate release at 75 μM ATP for RecBC unwinding and subsequent ssDNA translocation along the series of DNA substrates depicted schematically, that vary in duplex length L = 24, 29, 37, 40, 43, 48, 53, and 60 bp, with a constant $(dT)_{40}$ 3′-ssDNA extension. Phosphate release kinetics were measured using the fluorescent phosphate binding protein in Buffer M at 25°C as described in the text and Materials and Methods. The smooth curves are simulations based on the best fit parameters of each time course to Eq. (1) (see Table 1). (a inset)- Plot of the burst phase amplitude as a function of duplex DNA length. Smooth line is a linear fit to the data ([Pi] = 0.9549L + 45.079), yielding an average of 0.96±0.08 ATP/bp unwound. (b). DNA unwinding time courses under the same solution conditions and low [ATP]. Solid lines simulations based on the best fit parameters using Eq. (2) and the n-step sequential model Scheme 1. RecBC unwinds DNA with a rate of mk_{obs} = 114±4 bp/s at 75 μM ATP.

Table 1

Summary of phosphate release kinetics during RecBC unwinding and translocation[a]. Phosphate release time courses were fit to Eq.(1) and the burst amplitude (A_{burst}), burst rate (k_{burst}), and the steady-state rate (k_{ss}) are listed for each DNA length (L).

Simultaneous translocation along twin ssDNA extensions	A_{burst} **(Pi/RecBC)**	k_{burst} **(s^{-1})**	k_{ss} **(s^{-1})**	**c = 1.07 ± 0.09 ATP/nt**
L = 15 nt	48 ± 1	2.48 ± 0.17	4.09 ± 0.14	
30 nt	69 ± 2	2.31 ± 0.06	4.57 ± 0.11	
45 nt	82 ± 2	2.28 ± 0.05	5.05 ± 0.07	
60 nt	95 ± 1	2.15 ± 0.06	5.54 ± 0.18	
75 nt	115 ± 7	2.08 ± 0.09	6.03 ± 0.13	
Primary RecBC translocase only	A_{burst} **(Pi/RecBC)**	k_{burst} **(s^{-1})**	k_{ss} **(s^{-1})**	**c = 0.81 ± 0.05 ATP/nt**
L = 15 nt	44 ± 1	2.41 ± 0.16	4.51 ± 0.17	
30 nt	55 ± 1	2.34 ± 0.09	4.98 ± 0.12	
45 nt	71 ± 2	2.21 ± 0.06	5.75 ± 0.06	
60 nt	81 ± 3	2.13 ± 0.05	6.28 ± 0.15	
75 nt	92 ± 2	2.07 ± 0.03	7.13 ± 0.08	
Secondary RecBC translocase only	A_{burst} **(Pi/RecBC)**	k_{burst} **(s^{-1})**	k_{ss} **(s^{-1})**	**c = 1.12 ± 0.06 ATP/nt**
L = 15 nt	56 ± 1	2.51 ± 0.14	4.64 ± 0.09	
30 nt	81 ± 2	2.46 ± 0.07	5.02 ± 0.07	
45 nt	95 ± 1	2.31 ± 0.05	5.85 ± 0.16	
60 nt	108 ± 3	2.23 ± 0.03	6.57 ± 0.13	
75 nt	127 ± 3	2.10 ± 0.05	7.22 ± 0.15	
RecBC Unwinding	A_{burst} **(Pi/RecBC)**	k_{burst} **(s^{-1})**	k_{ss} **(s^{-1})**	**c = 0.95 ± 0.08 ATP/bp**
L = 24 bp	72 ± 2	1.99 ± 0.13	3.98 ± 0.14	
29 bp	78 ± 3	1.81 ± 0.06	4.27 ± 0.11	
37 bp	85 ± 1	1.53 ± 0.09	4.65 ± 0.08	
40 bp	87 ± 1	1.32 ± 0.05	5.56 ± 0.17	
43 bp	90 ± 2	1.14 ± 0.06	5.92 ± 0.14	
48 bp	95 ± 3	1.12 ± 0.04	6.29 ± 0.15	
53 bp	103 ± 4	0.90 ± 0.05	7.83 ± 0.08	
60 bp	113 ± 3	0.82 ± 0.03	7.96 ± 0.11	

[a]Time courses were fit to Equation (1) to obtain A_{burst}, k_{burst} and k_{ss}. Although k_{ss} increases with increasing DNA length, this does not affect the values of A_{burst} obtained from the fit to Eq. (1).